THE JOURNAL OF BIOLOGICAL CHEMISTRY VOL. 287, NO. 53, pp. 44561–44567, December 28, 2012

Characterization of Patient Mutations in Human Persulfide Dioxygenase (ETHE1) Involved in H_2S Catabolism*

Received for publication, August 2, 2012, and in revised form, November 9, 2012 Published, JBC Papers in Press, November 9, 2012, DOI 10.1074/jbc.M112.407411

Omer Kabil and Ruma Banerjee[1]

From the Department of Biological Chemistry, University of Michigan Medical Center, Ann Arbor, Michigan 48109-0600

Background: ETHE1 converts persulfides to sulfite in the mitochondrial sulfide oxidation pathway.
Results: The kinetics of human ETHE1 and two mutants described in patients have been characterized.
Conclusion: Both glutathione and coenzyme A serve as persulfide carriers for ETHE1, albeit with different efficacies.
Significance: Low steady-state H_2S levels are maintained by its efficient oxidation, and patient mutations in ETHE1 impair this activity.

Hydrogen sulfide (H_2S) is a recently described endogenously produced gaseous signaling molecule that influences various cellular processes in the central nervous system, cardiovascular system, and gastrointestinal tract. The biogenesis of H_2S involves the cytoplasmic transsulfuration enzymes, cystathionine β-synthase and γ-cystathionase, whereas its catabolism occurs in the mitochondrion and couples to the energy-yielding electron transfer chain. Low steady-state levels of H_2S appear to be controlled primarily by efficient oxygen-dependent catabolism via sulfide quinone oxidoreductase, persulfide dioxygenase (ETHE1), rhodanese, and sulfite oxidase. Mutations in the persulfide dioxgenase, *i.e.* ETHE1, result in ethylmalonic encephalopathy, an inborn error of metabolism. In this study, we report the biochemical characterization and kinetic properties of human persulfide dioxygenase and describe the biochemical penalties associated with two patient mutations, T152I and D196N. Steady-state kinetic analysis reveals that the T152I mutation results in a 3-fold lower activity, which is correlated with a 3-fold lower iron content compared with the wild-type enzyme. The D196N mutation results in a 2-fold higher K_m for the substrate, glutathione persulfide.

Ethylmalonic encephalopathy (EE),[2] an autosomal recessive disorder, is associated with a complex pathology affecting the brain, gastrointestinal tract, and peripheral vessels (1, 2). Patients with EE exhibit neurodevelopmental delay, acrocyanosis, relapsing petechiae, chronic diarrhea, and necrotic lesions in the deep gray matter and usually succumb to the disease within the first decade of life. The biochemical features associated with EE include elevated C4 and/or C5 acylcarnitines and lactic acid in blood, high urinary ethylmalonic acid, and cytochrome *c* oxidase deficiency in muscle and brain. The genetic locus culpable for EE-causing mutations was identified relatively recently and its gene product described as ETHE1 (3). More than 20 pathogenic mutations in ETHE1 have been described in EE patients (3). ETHE1 belongs to the metallo-β-lactamase superfamily (4) and is most similar to the glyoxylase II proteins (5), involved in detoxification of 2-oxoaldehydes. However, unlike glyoxylase II, which contains a dinuclear metal center that binds zinc, iron, or manganese (6–10), ETHE1 has a mononuclear iron in its active site (5).

The existence in microbes of ETHE1 variants fused to rhodanese or thiosulfate thioltransferase (5) and the elevated excretion of thiosulfate in ETHE1$^{-/-}$ mice and in EE patients (11) suggest involvement of this protein in sulfur catabolism. Indeed, recombinant human ETHE1 expressed in human HeLa cells or in *Escherichia coli* exhibits sulfur-dependent oxygenase activity as evidenced by oxygen consumption in the presence of the co-substrate, glutathione persulfide (GSSH) (equation 1) (11).

$$RSSH + O_2 + H_2O \rightarrow RSH + SO_3^{2-} + 2H^+ \qquad \text{(Eq. 1)}$$

Based on these results, ETHE1 was proposed to be a sulfur dioxgenase, which catalyzes the second step in the mitochondrial sulfide oxidation pathway downstream of sulfide quinone oxidoreductase (Fig. 1) (12). The latter oxidizes H_2S to persulfide and transfers electrons to the electron transport chain via reduced quinone (Fig. 1). Transfer of the persulfide from sulfide quinone oxidoreductase to glutathione or some other acceptor provides ETHE1 with its persulfide substrate that is oxidized to sulfite. Next, rhodanese catalyzes the conversion of 2 mol of sulfite to thiosulfate. Alternatively, sulfite can be oxidized to sulfate via the action of sulfite oxidase.

Steady-state tissue concentrations of H_2S are generally in the low nanomolar range (13, 14). One mechanism by which these low concentrations are maintained is via the efficient removal of H_2S by the sulfide oxidation pathway (15). It is estimated that H_2S concentrations $\geq$10–20 nM in the vicinity of mitochondria or 0.5–1 μM outside the cell stimulate its catabolism (15). By contrast, inhibition of cytochrome *c* oxidase by H_2S occurs at substantially higher H_2S concentrations: ~0.3 μM in cell homogenates and ~20 μM in intact cells (15, 16). Under hypoxic conditions, H_2S levels are expected to rise as oxygen-dependent catabolism slows. Conversely, high H_2S is expected to stimulate oxygen consumption leading to reduced oxygen concentrations. The interconnection between H_2S catabolism and oxy-

* This work was supported, in whole or in part, by National Institutes of Health Grant HL58984.
[1] To whom correspondence should be addressed: 3320B MSRB III, 1150 W. Medical Center Dr., University of Michigan, Ann Arbor, MI 48109-0600. Tel.: 734-615-5238; E-mail: rbanerje@umich.edu.
[2] The abbreviations used are: EE, ethylmalonic encephalopathy; GSSG, oxidized glutathione; GSSH, glutathione persulfide.

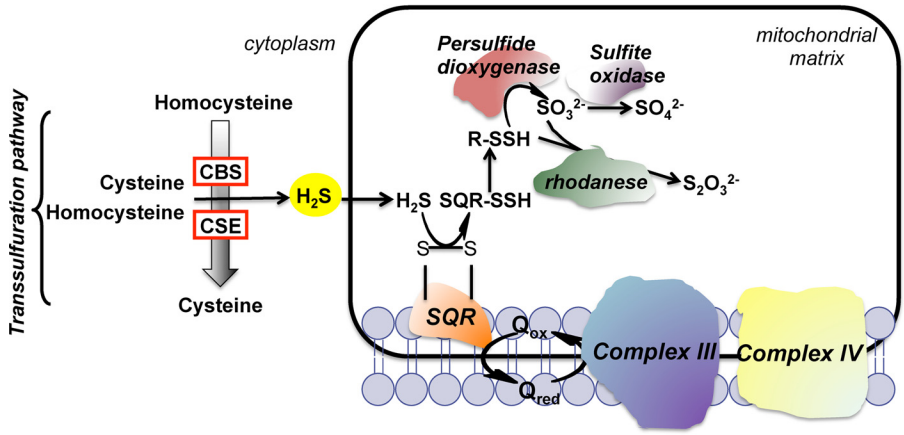

FIGURE 1. **Scheme showing pathways for H_2S biogenesis and degradation.** The transsulfuration pathway enzymes, cystathionine β-synthase (*CBS*) and γ-cystathionase (*CSE*) are primarily responsible for production of H_2S whereas the mitochondrial sulfide oxidation pathway handles its catabolism. SQR denotes sulfide quinone oxidoreductase, which oxidizes H_2S to persulfide, which is initially bound to an active site cysteine (denoted as SQR-SSH). It is not known if sulfide quinone oxidoreductase either directly, or via a small molecule acceptor *e.g.* glutathione or coenzyme A, transfers the persulfide to the next enzyme, persulfide dioxygenase.

gen has led to the proposal that H_2S is important for oxygen sensing (17, 18).

The structure of ETHE1 from *Arabidopsis thaliana* (58% sequence identity and >70% similarity with human ETHE1) reveals a dimeric protein with iron anchored via two histidines, one aspartate, and three water molecules (5). This coordination geometry resembles the 2-His-1-carboxylate facial triad seen in mononuclear nonheme iron(II) oxygenases (19). Although the residues that ligate the second metal in the dinuclear site of glyoxylases are also present in ETHE1, structural rearrangements appear to preclude their use for metal binding. Glyoxylases I and II catalyze the oxidation of 2-oxoaldheydes to hydroxyacids using glutathione as a cofactor. Like glyoxylase II, which binds *S*-D-lactoylglutathione (and hydrolyzes it to lactate and glutathione (8)), the active site of ETHE1 appears to be commodious enough for glutathione. However, it is substantially less spacious than the glyoxylase II active site particularly in the region that binds the thioester (5), consistent with the need to accommodate the smaller persulfide substituent. Indeed, ETHE1 does not hydrolyze *S*-D-lactoylglutathione and other glutathione thioesters (3, 20).

Given the importance of the sulfide oxidation pathway to H_2S homeostasis and possibly, the hypoxic response, it is important to understand the reaction mechanisms and regulation of the component enzymes. In this study, we report the first steady-state kinetic characterization of wild-type human persulfide dioxygenase (ETHE1) and two pathogenic variants, T152I and D196N, reported in EE patients (21).

EXPERIMENTAL PROCEDURES

Expression and Purification of Human Persulfide Dioxygenase—Recombinant human ETHE1 missing the N-terminal mitochondrial leader peptide was expressed in the *E. coli* strain BL21(DE3), using an expression plasmid (11) generously provided by Dr. Valeria Tiranti (IRCCS Foundation, Milan). The expressed protein contains a His_6 tag at the C terminus. An overnight 200-ml Luria Bertani (LB) culture, grown at 27 °C, was used to inoculate 6 liters of LB medium, and the cultures were supplemented with ferrous sulfate to a final concentration of 250 μM. When the A_{595} reached 0.4, ETHE1 expression was induced by adding 1 mM isopropyl-β-D-thiogalactopyranoside and cultured for an additional 12 h at 27 °C. Cells were harvested by centrifugation at 10,000 × *g* for 15 min at 4 °C.

ETHE1 was purified as follows. A cell pellet from a 6-liter culture was resuspended in 400 ml of 25 mM sodium phosphate buffer, pH 7.4 (Buffer A), supplemented with 0.5 M NaCl and 0.1% Tween 20, 1 tablet of complete protease inhibitor (Roche Applied Science), and 50 mg of lysozyme (Sigma). To the cell suspension, 35 mg of DNase (Sigma) and $MgCl_2$ to a final concentration of 10 mM were added and stirred at 4 °C for 30 min followed by sonication (Ultrasonic Processor XL) on ice using a macrotip with a pulse sequence of 30-s burst, 1-min rest with an output power setting of 7 (6-min total burst time). The cell lysate was centrifuged at 10,000 × *g* for 20 min. The supernatant was diluted 2-fold with Buffer A and loaded on a nickel-nitrilotriacetic acid fast flow column (Qiagen) equilibrated with the same buffer. After washing with 500 ml of Buffer A containing 20 mM imidazole, ETHE1 was eluted with a linear gradient ranging from 20 to 400 mM imidazole. Fractions containing ETHE1 at a purity of >95% were pooled and dialyzed overnight against 50 mM Tris, pH 8, and stored at −80 °C. Protein concentrations were determined using the Bradford reagent (Bio-Rad) with bovine serum albumin as a standard.

Preparation of Persulfide Substrates—Glutathione persulfide was prepared nonenzymatically by reacting NaHS and oxidized glutathione (GSSG) in a Coy anaerobic chamber (with a 95:5 atmosphere of N_2:H_2) (Equation 2).

$$NaHS + GSSG \rightarrow GSSH + GSH \qquad \text{(Eq. 2)}$$

An anaerobic solution of GSSG (20–50 mM in 300 mM sodium phosphate, pH 7.4, was mixed with a 4-fold excess of solid NaHS. The vial containing the reaction mixture was sealed immediately to prevent escape of H_2S and incubated at 37 °C for 30 min. The GSSH concentration was determined by cyanolysis of sulfane sulfur using the cold cyanolysis assay and colorimetric detection of the resulting ferric thiocyanate complex, as described previously (22). The persulfides of cysteine,

homocysteine, and coenzyme A were prepared using the same strategy.

Enzyme Assays—ETHE1 activity was measured using a polarographic oxygen consumption assay. The complete reaction mixture contained 100 mM sodium phosphate buffer, pH 7.4, 700 μM GSSH (standard assay), and ETHE1 (1–3 μg) in a total volume of 1.5 ml in a Gilson type chamber equipped with a Clark oxygen electrode and a magnetic stirrer at room temperature. The reactions were started by injection of substrate, and oxygen consumption was recorded on a Kipp and Zonen BD single channel chart recorder. The rate of oxygen consumption was expressed as μmol of O_2 min^{-1} mg of $protein^{-1}$ at 22 °C. We note that all assays had GSH at a concentration equal to GSSG as a consequence of the method of substrate preparation (Equation 2). The effect of GSH on the activity of ETHE1 was assessed in a separate assay by adding GSH to a final concentration of 5 mM. Alternative sulfur-containing compounds were tested as possible substrates at the following concentrations: 700 μM cysteine persulfide (+700 μM cysteine), 700 μM homocysteine persulfide (+700 μM homocysteine), 360 μM CoA persulfide (+360 μM CoA), 5 mM thiosulfate, and 5 mM GSH.

Metal Analysis—Plasma emission spectroscopy was used to analyze preparations of wild-type and mutant persulfide dioxygenases for their total metal content at the Chemical Analysis Laboratory, University of Georgia, Athens. Twenty metal ions, including the common transition metals, are detected by this method.

Gel Filtration Analysis—The native molecular mass of human ETHE1 was determined using a Sephadex G-250 column calibrated with standards from Bio-Rad. ETHE1 (0.5 ml of 12 mg/ml in 20 mM sodium phosphate buffer, pH 7.4) was loaded on the column equilibrated with the same buffer at 4 °C, and eluted at a flow rate of 0.5 ml min^{-1}. Protein was detected by absorption at 280 nm.

Thermal Denaturation Assays—The relative stabilities of the wild-type and mutant ETHE1 were assessed by thermal denaturation experiments. For this, 0.5 mg/ml purified protein in 100 mM HEPES, pH 7.4, in a total volume of 200 μl was placed in a quartz cuvette, and the temperature was increased from 25 to 70 °C in 5 °C increments, in a Cary 100 Bio UV/visible spectrophotometer equipped with a heating block connected to a water bath (Fisher Scientific Isotemp 3016S). Denaturation was monitored by an increase in absorbance at 600 nm at a given temperature until no further change in the optical density was observed.

HPLC Analysis of the ETHE1 Reaction—Stock solutions of the following standards: glutathione, thiosulfate, sulfite, NaHS, and GSSH, were prepared in 20 mM sodium phosphate buffer, pH 7.4. A stock solution of 60 mM monobromobimane (Invitrogen) was prepared in dimethyl sulfoxide and stored at −20 °C. Bimane adducts of standards were prepared in 20 mM sodium phosphate buffer, pH 7.4 (200-μl total volume), containing a 250 μM concentration of the standard compound and 1 mM monobromobimane incubated at room temperature for 10 min, and the reaction was terminated with 100 μl of 0.2 N sodium citrate, pH 2.0. Samples were protected from light during all the steps. The products of the ETHE1-catalyzed reaction were analyzed using the following reaction mixture: 250 μM GSSH, 250 μM GSH, and 2 μg of purified ETHE1 in 20 mM sodium phosphate buffer, pH 7.4 (total volume, 200 μl). The reaction mixture was incubated at room temperature for 5 min. Monobromobimane was then added to a final concentration of 1 mM, and incubation was continued for 10 min before acidification with sodium citrate as described above. A control reaction lacking ETHE1 was prepared in parallel. The derivatized samples were centrifuged at 10,000 × *g* for 10 min at 4 °C, and the supernatants were separated on a C8 reverse phase HPLC column (4.6 × 150 cm, 3 μm packing, Phenomenex) at room temperature using an Agilent 1100 series HPLC system equipped with a multisignal fluorescence detector. The sample (50 μl) was injected into the column equilibrated with a solution containing 80% Solvent A (100 ml of methanol, 897.5 ml of water, and 2.5 ml of acetic acid) and 20% Solvent B (900 ml of methanol, 97.5 ml of water, and 2.5 ml of acetic acid) and resolved using a gradient of Solvent B (20% from 1 to 10 min, 20–40% from 10 to 25 min, 40–90% from 25 to 30 min, 90–100% from 30 to 32 min, 100% from 32 to 35 min, 100–8% from 35 to 37 min, 8% from 37 to 45 min). The flow rate was 0.75 ml/min. Bimane adducts were detected by excitation at 340 nm and emission at 450 nm.

Electrospray Ionization Mass Spectroscopy Analysis—HPLC fractions corresponding to the elution peaks of interest were collected and submitted to the Mass Spectrometry Core Facility, Chemistry Department, University of Michigan.

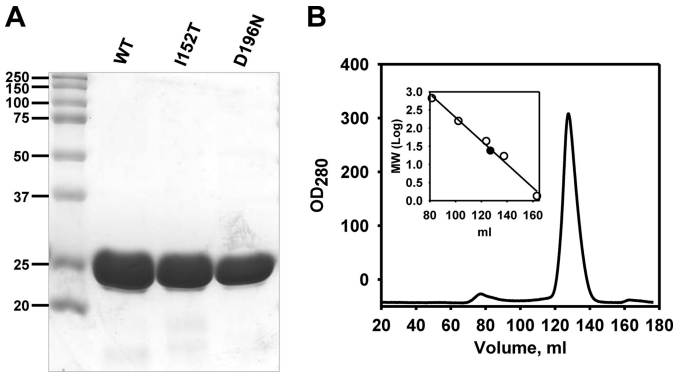

FIGURE 2. **Human ETHE1 is a monomeric protein.** *A*, ETHE1 (40 μg) was separated by SDS-PAGE and was judged to be >95% pure. The molecular mass markers are shown in the *left lane*. *B*, elution profile of ETHE1 from a gel filtration column reveals that it behaves as a monomeric protein.

RESULTS

Purification and Characterization of Persulfide Dioxygenase—We used a one-step protocol to purify recombinant human ETHE1 to >95% purity (Fig. 2*A*). The yield was ~75 mg of purified protein/liter of culture for both wild-type and mutant (T152I and D196N) proteins. The molecular mass of the recombinant proteins lacking the N-terminal 11-amino acid leader sequence was 25 kDa, based on SDS-PAGE analysis, consistent with the size predicted from its sequence (27.8 kDa). Wild-type and mutant purified persulfide dioxygenases eluted as single peaks from a size exclusion column with a retention time corresponding to 28 kDa, indicating that it exists as a monomer in solution (Fig. 2*B*).

Metal Analysis—The metal content of the wild-type and mutant proteins was determined by plasma emission spectroscopy. For wild-type protein, 0.82 mol of iron/mol of enzyme was obtained (Table 1). Both patient mutations resulted in

TABLE 1

Comparison of the kinetic properties of wild-type and mutant ETHE1

The kinetic parameters were determined by monitoring oxygen consumption in the presence of GSSH and either an equimolar amount of GSH (or 5 mM GSH) as described under "Experimental Procedures." Reactions were performed in 100 mM sodium phosphate buffer, pH 7.4, and contained 1–3 μg of enzyme.

ETHE1	Iron content	V_{max}	K_m	k_{cat}	k_{cat}/K_m
	mol Fe/ mol ETHE1	μ*mol min*$^{-1}$ *mg*$^{-1}$	*mM*	s^{-1}	$mM^{-1}\ s^{-1}$
Wild type	0.82	113 ± 4	0.34 ± 0.03	47	140
Wild type[a]	0.82	251 ± 11	0.25 ± 0.03	104	416
T152I	0.33	29.0 ± 1.3	0.31 ± 0.05	12	39
D196N	0.60	99.0 ± 3.8	0.74 ± 0.07	41	56

[a] 5 mM GSH.

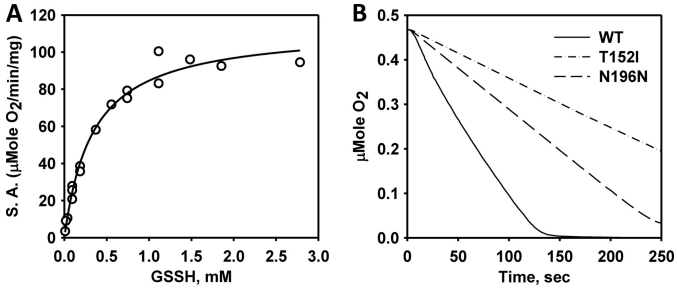

FIGURE 3. **Kinetic analysis of ETHE1.** *A*, dependence of the reaction velocity on substrate concentration for wild-type ETHE1. These data were obtained in the standard assay as described under "Experimental Procedures" with varying GSSH concentrations (in the presence of an equimolar GSH concentration). *B*, the activity of wild-type and mutant proteins was monitored by the rate of oxygen consumption in the presence of 500 μM GSSH and 500 μM GSH using an oxygen electrode.

TABLE 2

Alternative substrates for human ETHE1

The substrate concentrations used are described under "Experimental Procedures." Whenever a persulfide substrate was tested, an equimolar concentration of the corresponding thiol was present in the reaction mixture.

Substrate	Specific activity
	μ*mol min*$^{-1}$ *mg*$^{-1}$
GSSH	113.0 ± 4.0
CoA persulfide	2.4 ± 0.9
Cysteine persulfide	Not detectable
Glutathione	Not detectable
Thiosulfate	Not detectable

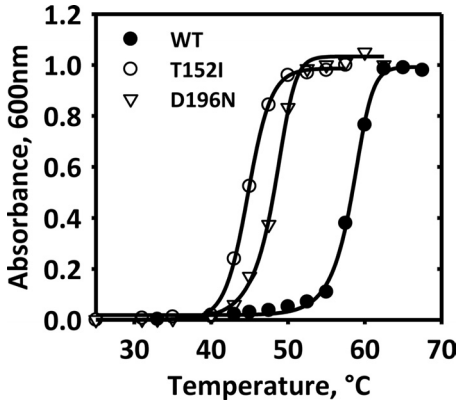

FIGURE 4. **Thermal stabilities of wild-type and mutant ETHE1.** Thermal melting curves for wild-type ETHE1 (*circles*), T152I (*triangles*), and D196N (*squares*). Protein unfolding was monitored spectrophotometrically at 600 nm as described under "Experimental Procedures."

lower iron content: 0.60 and 0.33 mol of iron/mol of D196N and T152I, respectively.

Kinetic Studies—An oxygen electrode was used to monitor the rate of oxygen consumption during conversion of GSSH to sulfite catalyzed by ETHE1. The specific activity of wild-type enzyme in the standard assay was 75 ± 8.8 μmol min^{-1} mg protein^{-1} at 22 °C (Fig. 3*A*). From the dependence of the reaction velocity on substrate concentration, a K_m for GSSH of 0.34 ± 0.03 mM and a V_{max} of 113 ± 4 μmol min^{-1} mg protein^{-1} was estimated for wild-type ETHE1 (Fig. 3*B*). Alternative small molecule persulfides and thiosulfate were tested as potential substrates for ETHE1. Neither cysteine persulfide nor thiosulfate resulted in detectable activity. In contrast, low activity was detected using 360 μM CoA persulfide as substrate (Table 2).

The T152I mutation resulted in an ~4-fold decrease in V_{max} (29 ± 1.3 μmol min^{-1} mg protein^{-1}) whereas the K_m for GSSH was unaffected by the mutation (308 ± 50 μM). The D196N mutation resulted in an ~15% decrease in V_{max} (99 ± 3.8) whereas the K_m for GSSH was ~2-fold higher (736 ± 72 μM) compared with wild-type enzyme.

Effect of GSH on ETHE1 Activity—Because the GSSH samples used in the enzyme assays bring in an equal concentration of GSH, the effect of the latter on ETHE1 was assessed. GSH is not a substrate for ETHE1, and oxygen consumption was not observed in its presence (Table 2). To assess the alternative possibility that GSH is an inhibitor of ETHE1, enzyme activity was measured at varying concentrations of GSSH and a single high, but physiologically relevant, concentration of GSH (5 mM). Under these conditions, a 2.2-fold increase in ETHE1 activity was observed compared with the standard assay containing 700 μM GSH and a saturating and equal concentration (700 μM) of GSSH. The K_m for GSSH was slightly lower (0.25 ± 0.03 mM) resulting in a 3-fold higher k_{cat}/K_m value. The activating effect of GSH on ETHE1 is presently not understood.

Stability of Wild-type and Mutant ETHE1—During purification, the T152I and D196N mutants appeared to be less stable than wild-type ETHE1, as evidenced by the propensity for precipitation during the concentration and dialysis steps. Comparison of the thermal denaturation profiles confirmed that both mutants are less stable than wild-type ETHE1 (Fig. 4). The T_m value of wild-type ETHE1 (59.8 ± 0.5 °C) was significantly higher than for the T152I (44.8 ± 0.05 °C) and D196N (49.8 ± 0.7 °C) enzymes.

Identification of Sulfite as the Product of the ETHE1-catalyzed Reaction—The derivatized reaction mixture was separated by HPLC, and peaks of interest were subjected to mass spectrometric analysis. In the presence of ETHE1, a new peak with a retention time of 18 min was observed (Fig. 5*A*), which was absent in the control sample lacking enzyme (Fig. 5*B*). The migration of the new peak coincided with the bimane adduct of a standard sulfite sample (Fig. 5*C*). The identity of sulfite was confirmed by mass spectrometric analysis in the negative ion mode that yielded a parent ion with an m/z value of 271.04,

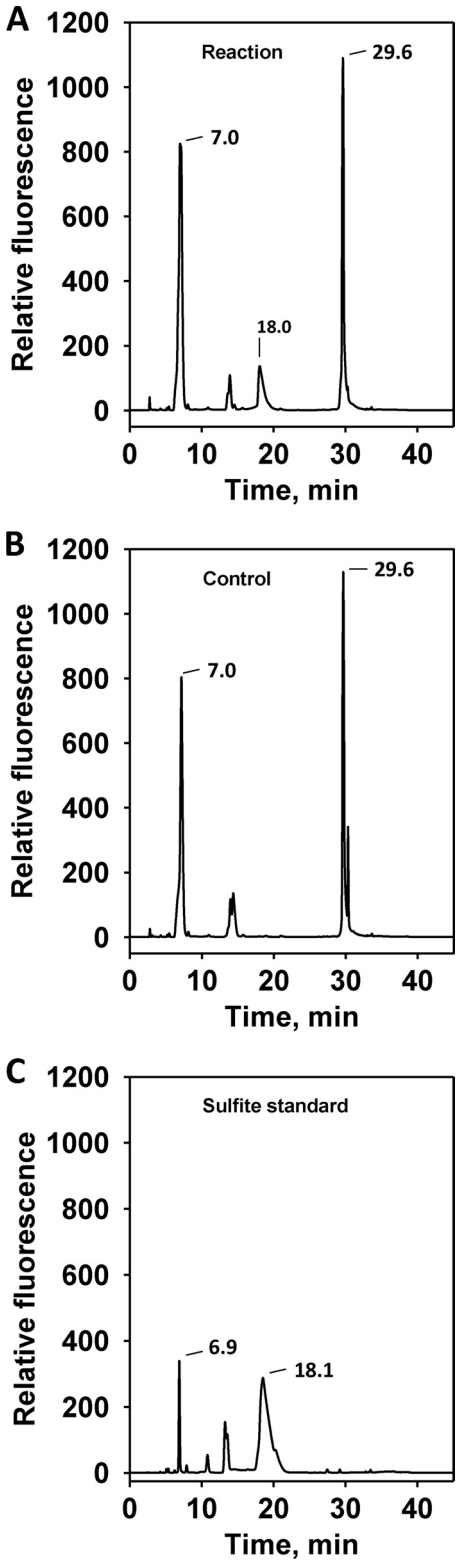

FIGURE 5. **HPLC analysis of sulfite generated by ETHE1.** *A*, a complete reaction containing 250 μM GSSH (250 μM GSH and H_2S) and 2 μg of enzyme was separated by HPLC using a C18 column as described under "Experimental Procedures." *B* and *C*, a control reaction mixture was set up as in *A* but lacked ETHE1 (*B*), and the bimane adduct of a sulfite standard was separated in *C*. The peak with a retention time of ~18 min represents sulfite and was seen in the reaction mixture (*A*) and in the sulfite standard (*C*), and its identity was confirmed by electrospray ionization mass spectrometry. The peaks at 29.65 min and ~7.0 min represent H_2S and a mixture of GSH (*A* and *B*) and a contaminant present in the monobromobimane (*C*), respectively.

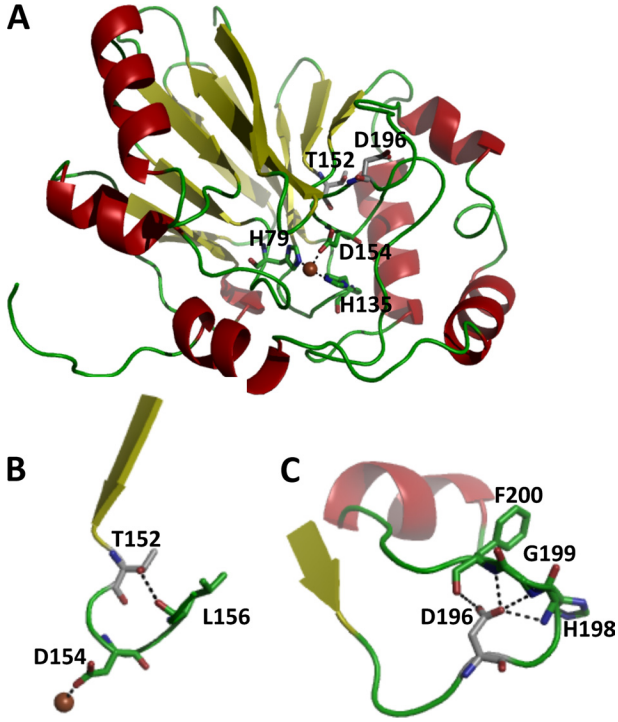

FIGURE 6. **Modeled structure of human ETHE1.** The structure was created using the *Arabidopsis* ETHE1 structure (Protein Database IC code 2GCU) as a template for the human ETHE1 sequence. *A*, the iron (*orange sphere*) ligands, His-79, Asp-154, and His-135, form the 2His:1Asp facial triad and are shown in *stick representation*. The locations of the two residues that are mutated in patients, Thr-152 and Asp-196, are indicated in *stick representation*. The location of the iron atom was obtained by overlaying the structure of the *Arabidopsis* ETHE1 on the modeled structure of the human protein. *B*, close-up shows the side chain interactions of Thr-152, which would be lost in the T152I mutation. The hydroxyl group of threonine interacts with the backbone carbonyl of Leu-156 stabilizing a bend in the loop. *C*, close-up shows the side chain interactions of Asp-196, which would be affected by the D196N mutation. One of the carboxylate oxygen atoms interacts with the backbone amide nitrogens of His-198, Gly-199, and Phe-200, whereas the other interacts with the backbone carbonyl oxygen of Phe-200. This network of electrostatic interactions is likely to important for positioning the loop.

which was identical to that obtained for the bimane adduct of a sulfite standard (data not shown). The retention times for the bimane adducts of GSH and sulfide which are also present in the reaction mixture were 7.0 and 29.6 min, respectively. The GSH-bimane peak (Fig. 5, *A* and *B*) co-elutes with a contaminant present in the derivatization mixture (Fig. 5*C*, retention time of 6.9 min).

Modeled Structure of Human Persulfide Dioxygenase—The structure of the *Arabidopsis* ETHE1 was used to generate a model of the human protein to obtain structural insights into the T152I and D196N mutations (Fig. 6). The modeled structure reveals that the active site iron is ligated by two histidines (His-79 and His-135 human sequence numbering) and one aspartate (Asp-154) (Fig. 6*A*). Whereas one of the residues that is mutated in a patient, Thr-152, is proximal to an iron ligand, Asp-154, the other, Asp-196 is distant from the active site. Both mutated residues reside on extended loops. The side chain of Thr-152 is engaged in a hydrogen bond interaction with the backbone carbonyl of Leu-156, closing off a turn in the loop (Fig. 6*B*). This interaction might be important for the optimal positioning of Asp-154, an iron ligand. Mutation of Thr-152 to isoleucine is predicted to lead to loss of this stabilizing interac-

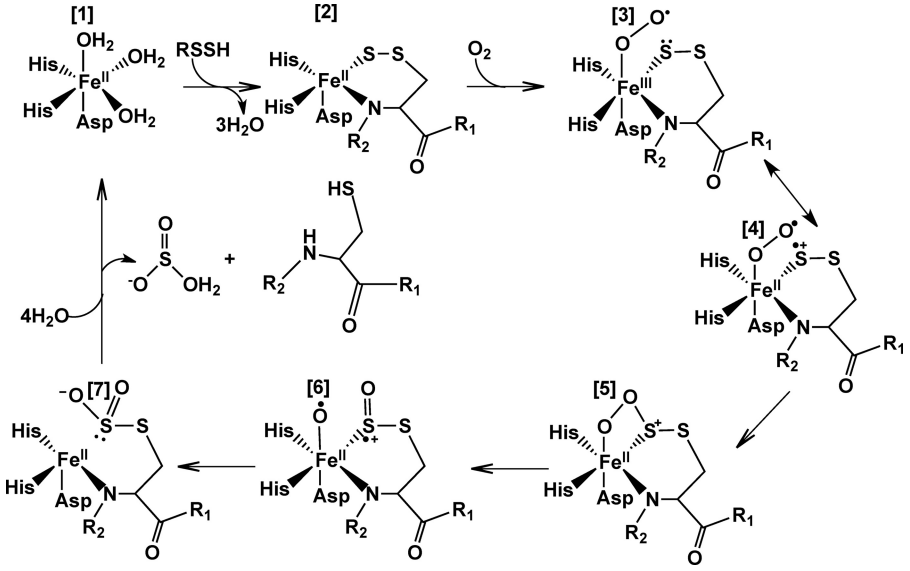

FIGURE 7. **Postulated reaction mechanism of ETHE1.** The reaction intermediates and mechanism was adapted from a proposal for the mechanistically related enzyme, cysteine dioxygenase (27). R_1 and R_2 in the GSSH substrate represent glutamate and glycine, respectively.

tion and is likely to be responsible for the 67% decrease in iron content and a corresponding decrease in V_{max} (Table 1).

The side chain of Asp-196, which appears to be quite distant from the active site, forms multiple interactions that appear to stabilize a turn in the loop on which it resides (Fig. 6*C*). Hence, one of the β-carboxylate oxygens of Asp-196 interacts with the backbone amide nitrogens of His-198, Gly-199, and Phe-200 whereas the other oxygen interacts with the backbone carbonyl oxygen of Phe-200. Mutation of Asp-196 to asparagine results in a 40% reduction in iron content and selectively impacts K_m for GSSH *versus* V_{max} (Table 1).

DISCUSSION

Nonheme iron dioxygenases are widely distributed in Nature and catalyze a diversity of oxidation reactions. These enzymes are important in biosynthetic, DNA repair, posttranslational modification, and catabolic pathways. The active site mononuclear iron is coordinated by 2His/1Asp(Glu) ligands, leaving open three sites that are occupied by water (Fig. 7, [**1**]). In ETHE1, a minimal mechanism involves displacement of water ligands upon substrate binding (shown as S and N coordination [**2**] followed by O_2 coordination to form an Fe(III)-superoxo complex [**3**]. The ligated sulfur acquires a partial radical cation character via resonance [**4**], and recombination with the Fe(II) superoxo ligand yields a cyclic peroxo intermediate [**5**]. Cleavage of the O-O bond forms a sulfoxy cation, and metal-bound activated oxygen [**6**] and subsequent transfer of the metal-bound activated oxygen [**7**] and hydrolysis yield sulfite. The tenets of this mechanism are currently under investigation using spectroscopic approaches.

Although ETHE1 exhibits activity with GSSH *in vitro*, its physiological substrate is not known. In principle, the persulfide bound in the active site peptide of sulfide quinone oxidoreductase might serve directly as a substrate for ETHE1 or indirectly, following transfer to a small molecule acceptor. The active site of ETHE1 appears to be sufficiently spacious to accommodate either GSSH or a short peptide from sulfide quinone oxidoreductase. In contrast, smaller persulfide carriers, *e.g.* cysteine and homocysteine that were tested in this study, do not appear to function as substrates for human ETHE1. In *ethe1*$^{-/-}$ mice, H_2S and thiosulfate levels are severalfold higher than in wild-type mice, sulfite is undetectable, and the activity of rhodanese, postulated to generate thiosulfate (12), is unaffected (11). Because rhodanese is postulated to be downstream of ETHE1 in the pathway (Fig. 1), the activity of ETHE1 as a GSSH dioyxgenase does not easily explain the clinical profile of EE patients, *i.e.* accumulation of thiosulfate and of C4 and C5 acylcarnitines. Because coenzyme A persulfide is a potent inhibitor of short chain acyl-CoA dehydrogenases (23, 24), we tested the hypothesis that it might serve as a substrate for ETHE1, thus explaining the observed accumulation of C4 and C5 acylcarnitines in patients. Our results indicate that CoA persulfide is a poor substrate for ETHE1, and the specific activity in its presence is ~2% that in the standard assay with GSSH. We note that due to the high cost, CoA persulfide was used at a final concentration of 360 μM versus 700 μM GSSH used in the standard assay. Thus, in the absence of information on the relative concentrations of GSSH versus coenzyme A persulfide in the mitochondrial matrix, the possibility that CoA serves as a physiologically relevant carrier for persulfide remains open.

Whereas a central role for thiosulfate in mammalian sulfide catabolism was suggested by early metabolic labeling studies (25), the formation and clearance of thiosulfate are poorly understood. Sulfite has been proposed to be a persulfide acceptor of sulfide quinone oxdioreductase generating thiosulfate as the product (26). Based on these studies, we tested the hypothesis that thiosulfate is an alternate substrate for ETHE1 and therefore accumulates in *ethe*$^{-/-}$ mice and in patients with EE. We proposed that thiosulfate can be catabolized to 2 mol of sulfite by Equation 3 or that glutathione rather than water displaces the terminal sulfur following its oxidation (Equation 4), and subsequent displacement of the second mole of sulfite from $GSSO_2H$ by water (Equation 5) completes the reaction. How-

ever, thiosulfate did not stimulate oxygen consumption and does not appear to be a substrate for ETHEI (Table 2).

$$S_2O_3^{2-} + O_2 + H_2O \rightarrow 2SO_3^{2-} + 2H^+ \quad \text{(Eq. 3)}$$

$$S_2O_3^{2-} + O_2 + GSH \rightarrow GSSO_2H + SO_3^{2-} \quad \text{(Eq. 4)}$$

$$GSSO_2H + H_2O \rightarrow SO_3^{2-} + 2H^+ + GSH \quad \text{(Eq. 5)}$$

An alternative explanation for the observed accumulation of thiosulfate in EE patients is that it is derived via the activity of cysteine dioxygenase, which oxidizes cysteine to cysteinesulfinic acid (27). The latter subsequently undergoes transamination to form β-sulfinylpyruvate, which decomposes to pyruvate and sulfite. We postulate that in the absence of a functional ETHE1, the persulfide generated by the activity of sulfide quinone oxidoreductase is preferentially consumed by rhodanese to form thiosulfate, explaining the clinically observed overproduction of this compound in EE patients.

In summary, we describe the first steady-state kinetic characterization of wild-type ETHE1 and two missense mutations identified in EE patients. The sulfide oxidation pathway is believed to play an important role in switching between low steady-state intracellular H_2S levels and the higher concentrations at which physiological effects of H_2S are elicited (28). The oxygen dependence of the ETHE1 reaction predicts that its activity will be limited under hypoxic conditions, suggesting one mechanism for accumulation of H_2S. Our studies provide the framework for evaluating the kinetics of H_2S clearance under normoxic versus hypoxic conditions.

Acknowledgments—We thank Dr. David Ballou (University of Michigan) for access to his oxygen electrode and Dr. Valerie Tiranti for providing the ETHE1 expression vector.

REFERENCES

1. Burlina, A., Zacchello, F., Dionisi-Vici, C., Bertini, E., Sabetta, G., Bennet, M. J., Hale, D. E., Schmidt-Sommerfeld, E., and Rinaldo, P. (1991) New clinical phenotype of branched-chain acyl-CoA oxidation defect. *Lancet* **338,** 1522–1523
2. García-Silva, M. T., Campos, Y., Ribes, A., Briones, P., Cabello, A., Santos Borbujo, J., Arenas, J., and Garavaglia, B. (1994) Encephalopathy, petechiae, and acrocyanosis with ethylmalonic aciduria associated with muscle cytochrome *c* oxidase deficiency. *J. Pediatr.* **125,** 843–844
3. Tiranti, V., D'Adamo, P., Briem, E., Ferrari, G., Mineri, R., Lamantea, E., Mandel, H., Balestri, P., Garcia-Silva, M. T., Vollmer, B., Rinaldo, P., Hahn, S. H., Leonard, J., Rahman, S., Dionisi-Vici, C., Garavaglia, B., Gasparini, P., and Zeviani, M. (2004) Ethylmalonic encephalopathy is caused by mutations in *ETHE1*, a gene encoding a mitochondrial matrix protein. *Am. J. Hum. Genet.* **74,** 239–252
4. Daiyasu, H., Osaka, K., Ishino, Y., and Toh, H. (2001) Expansion of the zinc metallohydrolase family of the β-lactamase fold. *FEBS Lett.* **503,** 1–6
5. McCoy, J. G., Bingman, C. A., Bitto, E., Holdorf, M. M., Makaroff, C. A., and Phillips, G. N., Jr. (2006) Structure of an ETHE1-like protein from *Arabidopsis thaliana*. *Acta Crystallogr. D Biol. Crystallogr.* **62,** 964–970
6. Cameron, A. D., Ridderström, M., Olin, B., and Mannervik, B. (1999) Crystal structure of human glyoxalase II and its complex with a glutathione thiolester substrate analogue. *Structure* **7,** 1067–1078
7. Crowder, M. W., Maiti, M. K., Banovic, L., and Makaroff, C. A. (1997) Glyoxalase II from *A. thaliana* requires Zn(II) for catalytic activity. *FEBS Lett.* **418,** 351–354
8. Zang, T. M., Hollman, D. A., Crawford, P. A., Crowder, M. W., and Makaroff, C. A. (2001) *Arabidopsis* glyoxalase II contains a zinc/iron binuclear metal center that is essential for substrate binding and catalysis. *J. Biol. Chem.* **276,** 4788–4795
9. Wenzel, N. F., Carenbauer, A. L., Pfiester, M. P., Schilling, O., Meyer-Klaucke, W., Makaroff, C. A., and Crowder, M. W. (2004) The binding of iron and zinc to glyoxalase II occurs exclusively as di-metal centers and is unique within the metallo-β-lactamase family. *J. Biol. Inorg. Chem.* **9,** 429–438
10. Marasinghe, G. P., Sander, I. M., Bennett, B., Periyannan, G., Yang, K. W., Makaroff, C. A., and Crowder, M. W. (2005) Structural studies on a mitochondrial glyoxalase II. *J. Biol. Chem.* **280,** 40668–40675
11. Tiranti, V., Viscomi, C., Hildebrandt, T., Di Meo, I., Mineri, R., Tiveron, C., Levitt, M. D., Prelle, A., Fagiolari, G., Rimoldi, M., and Zeviani, M. (2009) Loss of ETHE1, a mitochondrial dioxygenase, causes fatal sulfide toxicity in ethylmalonic encephalopathy. *Nat. Med.* **15,** 200–205
12. Hildebrandt, T. M., and Grieshaber, M. K. (2008) Three enzymatic activities catalyze the oxidation of sulfide to thiosulfate in mammalian and invertebrate mitochondria. *FEBS J.* **275,** 3352–3361
13. Furne, J., Saeed, A., and Levitt, M. D. (2008) Whole tissue hydrogen sulfide concentrations are orders of magnitude lower than presently accepted values. *Am. J. Physiol. Regul. Integr. Comp. Physiol.* **295,** R1479–1485
14. Levitt, M. D., Abdel-Rehim, M. S., and Furne, J. (2011) Free and acid-labile hydrogen sulfide concentrations in mouse tissues: anomalously high free hydrogen sulfide in aortic tissue. *Antioxid. Redox Signal.* **15,** 373–378
15. Bouillaud, F., and Blachier, F. (2011) Mitochondria and sulfide: a very old story of poisoning, feeding and signaling? *Antioxid. Redox Signal.* **15,** 379–391
16. Leschelle, X., Goubern, M., Andriamihaja, M., Blottière, H. M., Couplan, E., Gonzalez-Barroso, M. D., Petit, C., Pagniez, A., Chaumontet, C., Mignotte, B., Bouillaud, F., and Blachier, F. (2005) Adaptative metabolic response of human colonic epithelial cells to the adverse effects of the luminal compound sulfide. *Biochim. Biophys. Acta* **1725,** 201–212
17. Olson, K. R., Dombkowski, R. A., Russell, M. J., Doellman, M. M., Head, S. K., Whitfield, N. L., and Madden, J. A. (2006) Hydrogen sulfide as an oxygen sensor/transducer in vertebrate hypoxic vasoconstriction and hypoxic vasodilation. *J. Exp. Biol.* **209,** 4011–4023
18. Olson, K. R., and Whitfield, N. L. (2010) Hydrogen sulfide and oxygen sensing in the cardiovascular system. *Antioxid. Redox Signal.* **12,** 1219–1234
19. Hegg, E. L., and Que, L., Jr. (1997) The 2-His-1-carboxylate facial triad: an emerging structural motif in mononuclear nonheme iron(II) enzymes. *Eur. J. Biochem.* **250,** 625–629
20. Holdorf, M. M., Bennett, B., Crowder, M. W., and Makaroff, C. A. (2008) Spectroscopic studies on *Arabidopsis* ETHE1, a glyoxalase II-like protein. *J. Inorg. Biochem.* **102,** 1825–1830
21. Mineri, R., Rimoldi, M., Burlina, A. B., Koskull, S., Perletti, C., Heese, B., von Dobeln, U., Mereghetti, P., Di Meo, I., Invernizzi, F., Zeviani, M., Uziel, G., and Tiranti, V. (2008) Identification of new mutations in the *ETHE1* gene in a cohort of 14 patients presenting with ethylmalonic encephalopathy. *J. Med. Genet.* **45,** 473–478
22. Wood, J. L. (1987) Sulfane sulfur. *Methods Enzymol.* **143,** 25–29
23. Williamson, G., Engel, P. C., Mizzer, J. P., Thorpe, C., and Massey, V. (1982) Evidence that the greening ligand in native butyryl-CoA dehydrogenase is a CoA persulfide. *J. Biol. Chem.* **257,** 4314–4320
24. Shaw, L., and Engel, P. C. (1987) CoA-persulphide: a possible *in vivo* inhibitor of mammalian short-chain acyl-CoA dehydrogenase. *Biochim. Biophys. Acta* **919,** 171–174
25. Koj, A., Frendo, J., and Janik, Z. (1967) [^{35}S]Thiosulphate oxidation by rat liver mitochondria in the presence of glutathione. *Biochem. J.* **103,** 791–795
26. Jackson, M. R., Melideo, S. L., and Jorns, M. S. (2012) Human sulfide: quinone oxidoreductase catalyzes the first step in hydrogen sulfide metabolism and produces a sulfane sulfur metabolite. *Biochemistry* **51,** 6804–6815
27. McCoy, J. G., Bailey, L. J., Bitto, E., Bingman, C. A., Aceti, D. J., Fox, B. G., and Phillips, G. N., Jr. (2006) Structure and mechanism of mouse cysteine dioxygenase. *Proc. Natl. Acad. Sci. U.S.A.* **103,** 3084–3089
28. Vitvitsky, V., Kabil, O., and Banerjee, R. (2012) High turnover rates for hydrogen sulfide allow for rapid regulation of its tissue concentrations. *Antioxid. Redox Signal.* **17,** 22–31